

## Sensitivity-Enhanced Multiple-Quantum MAS NMR of Half-Integer Quadrupolar Nuclei<sup>†</sup>

T. Vosegaard,<sup>‡</sup> F. H. Larsen,<sup>‡,||</sup> H. J. Jakobsen,<sup>‡</sup>  
P. D. Ellis,<sup>§</sup> and N. C. Nielsen<sup>\*‡</sup>

Instrument Centre for Solid-State NMR Spectroscopy  
Department of Chemistry  
University of Aarhus  
DK-8000 Aarhus C, Denmark  
Environmental Molecular Sciences Laboratory  
Pacific Northwest National Laboratory  
Richland, Washington 99352

Received April 29, 1997

Revised Manuscript Received July 9, 1997

One of the most fascinating solid-state NMR experiments introduced within the past two years is the two-dimensional (2D) multiple-quantum (MQ) magic-angle spinning (MAS) experiment by Frydman and Harwood.<sup>1–14</sup> In an elegant and experimentally feasible manner this experiment accomplishes what earlier required technically more demanding methods, such as dynamic-angle spinning (DAS)<sup>15–17</sup> or double-rotation (DOR),<sup>17–19</sup> namely the achievement of high-resolution spectra of half-integer quadrupolar nuclei possessing large quadrupole coupling interactions. By combining the evolution of MQ and single-quantum (1Q) coherences, active in two different time periods of a 2D experiment, broadening by second-order quadrupolar coupling may be eliminated in one dimension ( $\omega_1$ ) while second-order broadened spectra are observed in the other ( $\omega_2$ ) dimension. In some cases preservation of resolved second-order lineshapes in the  $\omega_2$  dimension, from which the quadrupolar coupling parameters can be extracted, is of fundamental interest for determination of isotropic chemical shifts from the line positions in the high-resolution  $\omega_1$  dimension (influenced by second-order quadrupolar shifts). In other applications, where the determination of accurate isotropic chemical shifts is irrelevant, the high resolution of the isotropic  $\omega_1$  dimension may by itself provide the relevant information.

While there has been no dispute about the advantages of the MQMAS method in terms of resolution, improvement of the

sensitivity for the experiment has been addressed by several authors.<sup>2,3,5,6,10–12</sup> Two factors are important for the sensitivity of the experiment. First, the excitation of MQ coherences (MQC's) and their subsequent reconversion into 1QC for nuclei exhibiting large quadrupolar interactions are difficult and often subjected to low transfer efficiencies.<sup>20,21</sup> Second, indirect observation of the combined MQ and 1Q evolution ( $\omega_1$ ) through second-order quadrupolar broadened ( $-1$ )Q MAS lineshapes ( $\omega_2$ ) may significantly reduce the sensitivity of the experiment compared to that obtained by a hypothetical high-resolution experiment without second-order broadening in the  $\omega_2$  dimension. Several solutions to the first problem, including single-pulse excitation<sup>2,3,5,10</sup> or excitation using spin-lock sequences,<sup>11</sup> have been proposed. In contrast, the second problem has not yet been addressed.

In this Communication we present a new method which effectively improves the sensitivity of the MQMAS experiment by splitting the second-order quadrupolar lineshapes in the  $\omega_2$  dimension into manifolds of spin-echo "sidebands" while preserving high resolution in the  $\omega_1$  dimension. The timing scheme of our proposed MQ-QCPMG-MAS (MQ Quadrupolar Carr–Purcell–Meiboom–Gill<sup>22–25</sup> MAS) pulse sequence is presented in Figure 1 along with the coherence transfer pathways for an ensemble of  $I = 3/2$  quadrupolar nuclei. The  $p = 0 \rightarrow \pm 3 \rightarrow \pm 1 \rightarrow 0 \rightarrow \pm 1 \rightarrow \mp 1 \rightarrow$  etc. pathways are selected by selective rf pulses<sup>26</sup> and phase cycling.<sup>29</sup> The first pulse is tuned to efficiently excite the desired MQC which evolve during the first part ( $1/(1+k)$ ) of the  $t_1$  period. The second pulse transfers the MQC back to 1QC which after a period  $k t_1/(1+k)$  forms an echo with all anisotropic interactions refocused ( $k = 7/9$  for spin  $I = 3/2$  nuclei). The third and fourth pulse are selective<sup>26</sup>  $\pi/2$  pulses for the central transition and constitute a  $z$  filter,<sup>7,9</sup> which leads to an equal distribution of  $-1$ QC and  $+1$ QC. These coherences are refocused using a selective rotor-synchronized spin echo (fifth pulse) to prevent sampling close to a rf pulse. Finally, the free induction decay (FID) for the central ( $1/2, -1/2$ ) transition is sampled during a train of selective<sup>26</sup> refocusing  $\pi$  pulses which constitute the QCPMG part (cf., Figure 1a) of the pulse sequence. The QCPMG sequence is rotor synchronized according to  $2N\tau_r = \tau_a + 2\tau + \tau_\pi$  where  $2N$  is the number of rotor echoes per spin-echo period and  $1/\tau_a$  the spin-echo sideband separation. We note that a similar strategy based on CPMG<sup>22,23</sup> has earlier been proposed for sensitivity enhancement of 2D magic-angle hopping experiments for spin  $I = 1/2$  nuclei in static powder samples.<sup>30</sup> Sampling through the quadrupolar version<sup>24,25</sup> of the CPMG pulse sequence<sup>22,23</sup> (QCPMG) has recently been successfully exploited to record sensitivity-enhanced quadrupolar echo spectra for the central transition of half-integer quadrupolar nuclei in static powder<sup>31</sup> and MAS<sup>32</sup> experiments.

Figure 2 shows a series of <sup>23</sup>Na MQMAS and MQ-QCPMG-

<sup>†</sup> Presented at the 38th Experimental NMR Conference, Orlando, FL, March 1997.

<sup>‡</sup> University of Aarhus.

<sup>§</sup> Pacific Northwest National Laboratory.

<sup>||</sup> Present address: Environmental Molecular Sciences Laboratory, Pacific Northwest National Laboratory, Richland, WA 99352.

- (1) Frydman, L.; Harwood, J. S. *J. Am. Chem. Soc.* **1995**, *117*, 5367.
- (2) Medek, A.; Harwood, J. S.; Frydman, L. *J. Am. Chem. Soc.* **1995**, *117*, 12779.
- (3) Wu, G.; Rovnyak, D.; Sun, B.; Griffin, R. G. *Chem. Phys. Lett.* **1995**, *249*, 210.
- (4) Fernandez, C.; Amoureux, J.-P. *Chem. Phys. Lett.* **1995**, *242*, 449.
- (5) Fernandez, C.; Amoureux, J.-P. *Solid State NMR* **1996**, *5*, 315.
- (6) Massiot, D.; Touzo, B.; Trumeau, D.; Coutures, J. P.; Virlet, J.; Florian, P.; Grandinetti, P. *J. Solid State NMR* **1996**, *6*, 73.
- (7) Brown, S.; Heyes, S. J.; Wimperis, S. *J. Magn. Reson. A* **1996**, *119*, 280.
- (8) Fernandez, C.; Amoureux, J.-P.; Delmotte, L.; Kessler, H. *Microporous Mater.* **1996**, *6*, 125.
- (9) Amoureux, J.-P.; Fernandez, C.; Steuernagel, S. *J. Magn. Reson. A* **1996**, *123*, 116.
- (10) Amoureux, J.-P.; Fernandez, C.; Frydman, L. *Chem. Phys. Lett.* **1996**, *259*, 347.
- (11) Wu, G.; Rovnyak, D.; Griffin, R. G. *J. Am. Chem. Soc.* **1996**, *118*, 9326.
- (12) Duer, M. J.; Stourton, C. *J. Magn. Reson.* **1997**, *124*, 189.
- (13) Wu, G.; Kroeker, S.; Wasylishen, R. E.; Griffin, R. G. *J. Magn. Reson.* **1997**, *124*, 237.
- (14) Brown, S. P.; Wimperis, S. *J. Magn. Reson.* **1997**, *124*, 279.
- (15) Llor, A.; Virlet, J. *Chem. Phys. Lett.* **1988**, *152*, 248.
- (16) Mueller, K. T.; Sun, B. Q.; Chingas, G. C.; Zwanziger, J. W.; Terao, T.; Pines, A. *J. Magn. Reson.* **1990**, *86*, 470.
- (17) Chmelka, B. F.; Mueller, K. T.; Pines, A.; Stebbins, J.; Wu, Y.; Zwanziger, J. W. *Nature* **1989**, *339*, 42.
- (18) Samoson, A.; Lippmaa, E.; Pines, A. *Mol. Phys.* **1988**, *65*, 1013.
- (19) Wu, Y.; Sun, B. Q.; Pines, A.; Samoson, A.; Lippmaa, E. *J. Magn. Reson.* **1990**, *89*, 297.

(20) Vega, S.; Naor, Y. *J. Chem. Phys.* **1981**, *75*, 75.

(21) Nielsen, N. C.; Bildsøe, H.; Jakobsen, H. *J. Chem. Phys. Lett.* **1992**, *191*, 205; *J. Magn. Reson.* **1992**, *97*, 149.

(22) Carr, H. Y.; Purcell, E. M. *Phys. Rev.* **1954**, *94*, 630.

(23) Meiboom, S.; Gill, D. *Rev. Sci. Instrum.* **1958**, *29*, 688.

(24) Bloom, M.; Sternin, E. *Biochemistry* **1987**, *26*, 2101.

(25) Engelsberg, M.; Yannoni, C. S. *J. Magn. Reson.* **1990**, *88*, 393.

(26) In the limit of large quadrupole coupling constants ( $C_Q$ ) relative to the amplitude of the rf irradiation (i.e.,  $2\pi C_Q/[4I(I-1)\omega_{rf}] > 3$  where  $\omega_{rf}$  is the rf field strength) selective operation on the central transition ( $1/2, -1/2$ ) is accomplished by scaling of the pulse flip angles according to  $\theta = \theta_p/(I + 1/2)$  where  $\theta_p = \omega_{rf}\tau_p$  ( $\tau_p$  is the pulse duration) is the nominal pulse flip angle.<sup>21,27,28</sup>

(27) Abragam, A. *The Principles of Nuclear Magnetism*; Clarendon Press: Oxford, 1961.

(28) Schmidt, V. H. in *Proceedings Ampère Intl. Summer School II*, 1971; p 79.

(29) Bodenhausen, G.; Kogler, H.; Ernst, R. R. *J. Magn. Reson.* **1984**, *58*, 370.

(30) Szeverenyi, N. M.; Bax, A.; Maciel, G. E. *J. Magn. Reson.* **1985**, *61*, 440.

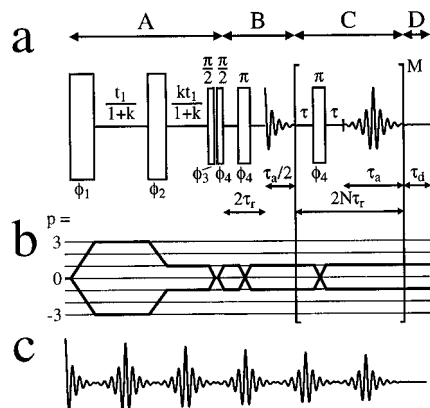


**Figure 1.** (a) Timing scheme of the MQ-QCPMG-MAS pulse sequence where the events during A, B, C, and D constitute a  $z$ -filtered MQMAS experiment,<sup>7,9</sup> a rotor-synchronized spin echo, the replicating part of the QCPMG sequence ( $N$ ,  $M$  integers), and an additional sampling period to ensure full decay of the FID. Part C is rotor-synchronized according to  $2N\tau_r = \tau_a + 2\tau + \tau_\pi$ , where  $\tau_\pi$  is the duration of the selective  $\pi$  pulse. (b) Coherence transfer pathway applied to an ensemble of spin  $I = 3/2$  nuclei and selected using  $\phi_j^i = 2\pi j/n_i$ ,  $j = 0, \dots, n_i - 1$ , with  $n_i = 6, 4, 2$ , and  $2$  (in given order) and the receiver reference phase adjusted to select the coherences indicated, according to standard procedures.<sup>29</sup> (c) Visualization of the FID recorded in the direct sampling dimension ( $t_2$ ) of the 2D experiment.

MAS spectra for an approximately equimolar sample of  $\text{Na}_2\text{SO}_4$  and  $\text{Na}_2\text{C}_2\text{O}_4$  (both anhydrous polycrystalline powders). Clearly, all spectra display well-resolved resonances for  $\text{Na}_2\text{SO}_4$  (34 ppm) and  $\text{Na}_2\text{C}_2\text{O}_4$  (40 ppm) in the  $\omega_1$  dimension of the 2D spectrum. Contrary, the appearance in the  $\omega_2$  dimension and the spectral sensitivity differ significantly for the five spectra depending on the sampling conditions in this dimension. The standard  $z$ -filtered MQMAS spectrum (Figure 2a) shows broad second-order quadrupolar lineshapes for the two  $^{23}\text{Na}$  resonances. Upon detection during a QCPMG train of selective  $\pi$  pulses these resonances split into manifolds of sidebands (Figures 2b–e) as a result of the combined action of spin and rotary echoes. Since the overall spectral intensity of the experiment is defined solely by the intensity of the first point of the free induction decay, decomposition of the spectrum into a set of distinct spin-echo sidebands translates directly into increased sensitivity of the experiment. By adjustment of the echo-sampling period  $\tau_a$ , it is feasible to specify the number of spin-echo sidebands and thereby the content of information in this dimension and the overall sensitivity of the experiment. For example, by increasing the sideband separation the sensitivity increases at the expense of the information about the inhomogeneous quadrupole coupling and chemical shielding interactions defining the envelope of the spin-echo sideband pattern. Information about homogeneous interactions (homonuclear dipolar coupling and dynamics) may independently be obtained from the line shape of the spin-echo sidebands being determined by sampling of multiple spin echoes. The spectra in Figure 2b–e correspond to gain factors in signal intensity of 5, 8, 12, and 20, respectively. It is evident that the spectrum of highest gain (Figure 2e with a separation  $1/\tau_a = 2$  kHz between sidebands) yields little information about the quadrupole interaction. This may be acceptable in applications where the main concern is resolution/determination of the number of different chemical sites. Decreasing the sideband separation from 2000 to 250 Hz in Figure 2 gradually introduces a manifold of spin-echo sidebands with an envelope resembling the standard  $z$ -filtered MQMAS spectrum. Thus, in principle the MQ-QCPMG-MAS spectrum in Figure 2b may provide the same

(31) Larsen, F. H.; Jakobsen, H. J.; Ellis, P. D.; Nielsen, N. C. Submitted for publication, 1997.

(32) Larsen, F. H.; Jakobsen, H. J.; Ellis, P. D.; Nielsen, N. C. Submitted for publication, 1997.

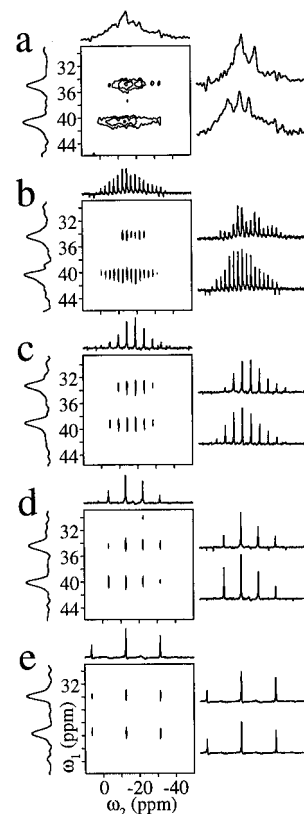


**Figure 2.** (a)  $^{23}\text{Na}$   $z$ -filtered MQMAS and (b–e) MQ-QCPMG-MAS 2D spectra of an approximately equimolar sample of anhydrous  $\text{Na}_2\text{SO}_4$  and  $\text{Na}_2\text{C}_2\text{O}_4$  polycrystalline powders. The spectra were recorded at 105.8 MHz using a Varian UNITY-400 spectrometer with a home-built high-speed spinning MAS probe using 5 mm  $\text{Si}_3\text{N}_4$  rotors. An rf field strength  $\omega_{\text{rf}}/2\pi = 58$  kHz was applied for all pulses. Pulse lengths of 20, 10, 2.2, 2.2, and 4.4  $\mu\text{s}$  were used for the pulses in the same order as shown in Figure 1a. Each spectrum has 96 scans, a relaxation delay of 3 s, 10  $\mu\text{s}$  dwell time during  $t_2$ , and 128  $t_1$  increments separated by 67  $\mu\text{s}$ . For the MQ-QCPMG-MAS spectra ( $\tau = 150$   $\mu\text{s}$ ) the number of points per echo (corresponding  $\tau_a$  value), numbers of replicating echos ( $M$ ), and MAS frequency were (b) 400 (4 ms), 9, 10.7 kHz; (c) 200 (2 ms), 19, 10.4 kHz; (d) 100 (1 ms), 39, 10.7 kHz; and (e) 50 (500  $\mu\text{s}$ ), 80, 9.9 kHz. The  $^{23}\text{Na}$  chemical shift scales (ppm) are relative to external 1.0 M NaCl.

information as the MQMAS spectrum in Figure 2a while simultaneously a 5-fold improvement in sensitivity is obtained.

In conclusion, the MQ-QCPMG-MAS experiment introduced here significantly improves the sensitivity of the extremely useful MQMAS experiment. This sensitivity gain is obtained solely by modifying the conditions in the sampling dimension. Therefore, it may be combined with schemes providing additional sensitivity improvement by more efficient MQC excitation and MQC to 1QC conversion. The actual gain in sensitivity depends on the desired definition of the second-order quadrupolar envelope of sidebands which paves the way for information about quadrupole coupling and shielding parameters and thereby second-order shifts required for determination of the isotropic chemical shifts.

**Acknowledgment.** The use of the Varian UNITY-400 NMR spectrometer, sponsored by Teknologistyrelsen, at the Instrument Centre for Solid-State NMR Spectroscopy, University of Aarhus, is acknowledged. Support of this research by equipment grants from the Danish Natural Science Research Council, Carlsbergfondet, and Aarhus University Research Foundation is acknowledged. This work has been supported in part by the National Institutes of Health under a Related Services Agreement with the U.S. Department of Energy (DOE) under contract DE-AC06-76RLS 1830, Federal Grant 8-R1GM26295F. Pacific Northwest National Laboratory is operated for DOE by Battelle.